Stress Field Analysis of Polymer Composite with Orthogonally Reinforced Fibers

Shweta Gupta[1,*], Parshant Kumar[2] and V.K. Srivastava[2]

[1]*Department of Mechanical Engineering, PDPM Indian Institute of Information Technology Design & Manufacturing, Jabalpur-482005, India*

[2]*Department of Mechanical Engineering, Indian Institute of Technology (BHU), Varanasi-221005, India*

Abstract: The photoelastic technique was used to analyze the stress field in glass fiber reinforced polymer matrix composite. Two glass fiber bundles with a diameter of 0.2 mm were reinforced in orthogonal directions. The composite was subjected to diametrical compression with two orientation of fibers with respect to the loading axis, i.e. $0^0/90^0$ and $45^0/135^0$. A circular polariscope with dark-field arrangement was used to analyze the stress field. The isochromatic fringe pattern nearby fiber/matrix interface revealed that there was strong adhesion between the fiber and matrix. Distorted fringes were observed nearby fiber region which indicated efficient load transfer from matrix to the fiber. It was observed that composite with $45^0/135^0$ orientation of fibers showed more principal stress difference in the direction perpendicular to the loading axis.

Keywords: Photoelastic analysis, polymer composite, stress analysis.

1. INTRODUCTION

Fiber-reinforced composites (FRC) exhibit excellent properties such as high specific strength, high resistance to fracture, fatigue, and corrosion due to which these composites are used in aerospace, aeronautical and automobile sectors [1]. The properties of FRC depend on the type of fiber, matrix, and fiber/matrix interface [2]. To tailor the properties of FRC, the fiber/matrix interface needs to be understood and engineered. Some researchers have used functionalization techniques to increase adhesion between fiber and matrix [3-6]. Functionalization improves the interfacial properties due to which load is transferred efficiently at the interface. To characterize the load transfer at the interface, several experimental as well as numerical techniques, have been developed [7, 8]. Photoelasticity is one of them [2].

Full stress field around fiber/matrix interface can be viewed at any stress level using photoelasticity. But the main limitation of photoelasticity lies in the type of materials to be investigated. Only birefringent materials can be characterized using photoelasticity. Isotropic materials are easy to characterize using photoelastic techniques because material fringe value does not vary with the orientation of the material. But in case of continuous FRC (orthotropic materials), fringe value varies with the orientation of fibers due to which it is a bit complex to characterize FRC using photo-elasticity.

In 1952, Cox [9] was the first who tried to analyze orthotropic material with birefringent matrix and reported fiber stress distribution along the fiber/matrix interface with both the matrix and the fiber undergoing elastic deformation. Sampson [10] also analyzed the orthotropic material by using photoelastic technique considering Mohr's circle relevance to obtain birefringent components.

Isoclinics and isochromatic fringes are usually obtained in the photoelastic method. Isoclinic angles and isochromatic fringe orders are assigned to the respective fringes. Isoclinic fringes are the bands of the constant angle of the principal stresses with the reference axis of polariscope. Isochromatic fringes represent the regions of constant principal stress difference. A dark field circular polariscope arrangement can be used to analyze the fiber/matrix interface [11]. Isoclinic fringes extinct in circular polariscope, thus only isochromatic fringes can be observed. Only integer values of fringe order can be obtained using dark-field arrangement whereas bright field arrangement can be used to obtain fractional fringe order.

The researchers who have characterized fiber/matrix interface using photoelastic analysis had mostly worked on unidirectional fiber-reinforced polymer composites [2, 10, 11]. There is lack of literature available on photoelastic analysis of bidirectionally reinforced FRC. The generation of stresses in bidirectionally fiber-reinforced composites is different from unidirectionally reinforced composites [12]. Thus, the present article focusses on the stress

Address correspondence to this article at the Department of Mechanical Engineering, PDPM Indian Institute of Information Technology Design & Manufacturing, Jabalpur-482005, India; Tel: +91-761-2794441;
Fax: +91-761-2632524; E-mail: shwetagupta888111@gmail.com

E-ISSN: 2410-4701/19

field analysis of the bidirectionally fiber reinforced polymer composites. Two orientations of fibers (i.e. $0^0/90^0$ and $45^0/135^0$) were considered in the present article. The results indicated that the reinforcement of fibers might influence the stress pattern to a significant extent.

2. MATERIALS AND METHODS

2.1. Material

To analyze compressive behavior, a disc type specimen was fabricated. The specimen contained epoxy as matrix and glass fibers as reinforcement which were reinforced along two diametrical axes and oriented at 90^0 to each other. A mold made of plaster of paris was prepared. Two glass fiber bundles were arranged in the mold at the desired locations. To fabricate composite, a standard DGEBA (diglycidyl ether of bisphenol-A) epoxy resin and a curing agent (hardener, PH861) were taken in a beaker in the ratio of 10:1 by weight. The epoxy was first mixed with hardener and stirred by a mechanical stirrer for 10 minutes to avoid any entrapment of air bubbles in the molded specimen. The liquid mixture was then poured into the mold and left for curing for about 16 hours. After curing in mold, the specimen was taken out from the mold and left for further curing in ambient atmosphere for about 30 hours. The diameter of the obtained disc type compressive specimen was 43 mm with a thickness of 5 mm. The two glass fibers were reinforced in two mutually perpendicular directions with a length of 43 mm. The diameter of each fiber bundle was 0.2 mm.

2.2. Experimental Set Up

Circular polariscope with dark-field arrangement was used in this analysis. Two polarizers and two quarter-wave plates were kept at crossed positions with respect to each other as shown in Figure **1**. 1st quarter-wave plate was placed 45^0 to the polarizing axis of polarizer. There are two axes in the quarter-wave plate named as fast and slow axis based on the difference in their refractive indices along these axes. The fast axis of 1st quarter-wave plate was parallel to slow axis of 2nd quarter-wave plate and vice versa. The specimen was placed in-between the two quarter-wave plates. The positions of polarizer and analyzer were 0^0 and 90^0 respectively. Sodium lamp was used as the monochromatic source of light. To get an idea about stress field distribution, images were captured when the respective fringes met at the center of disc. The schematic illustration showing the arrangement of circular polariscope and loading configuration is shown in Figure **1**.

2.3. Compression Test

The compression test was performed at different orientations of the glass fiber with respect to loading axis i.e. $0^0/90^0$ (F0) and $45^0/135^0$ (F45) as shown in the inset of Figure **1**. The load was increased gradually. The load values were noted when isochromatic fringes

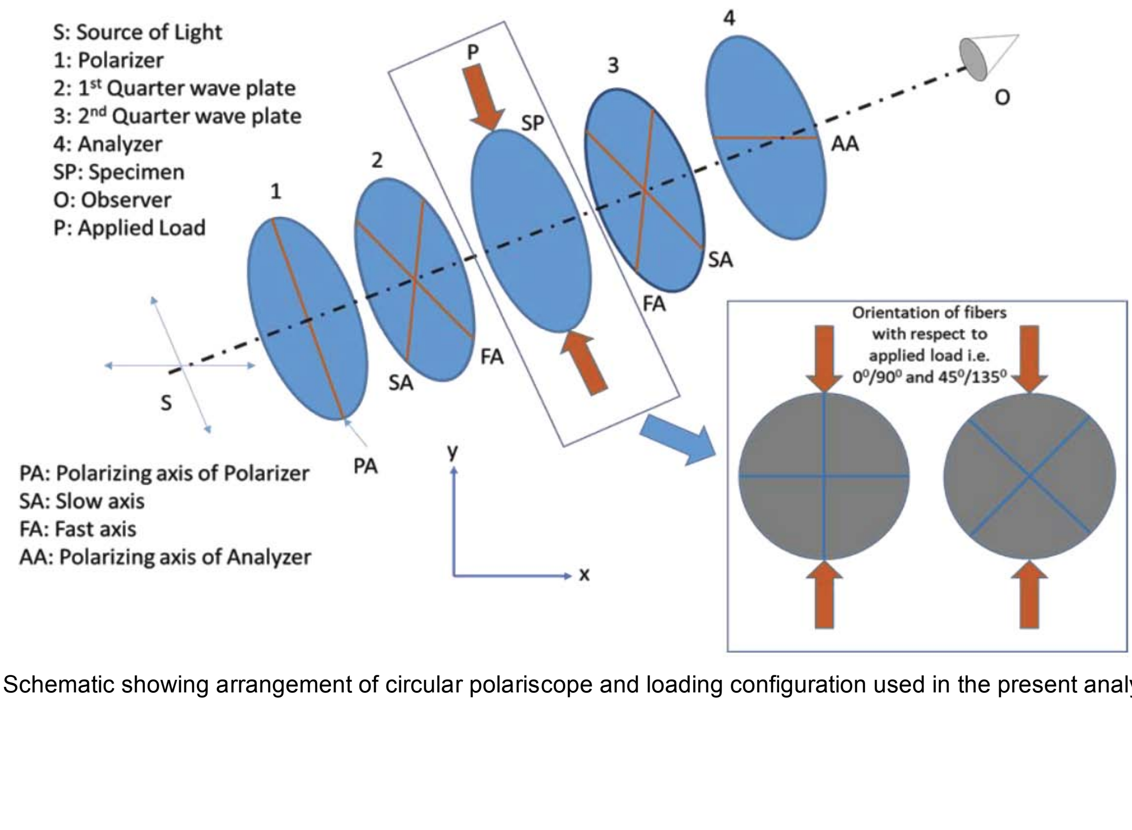

Figure 1: Schematic showing arrangement of circular polariscope and loading configuration used in the present analysis.

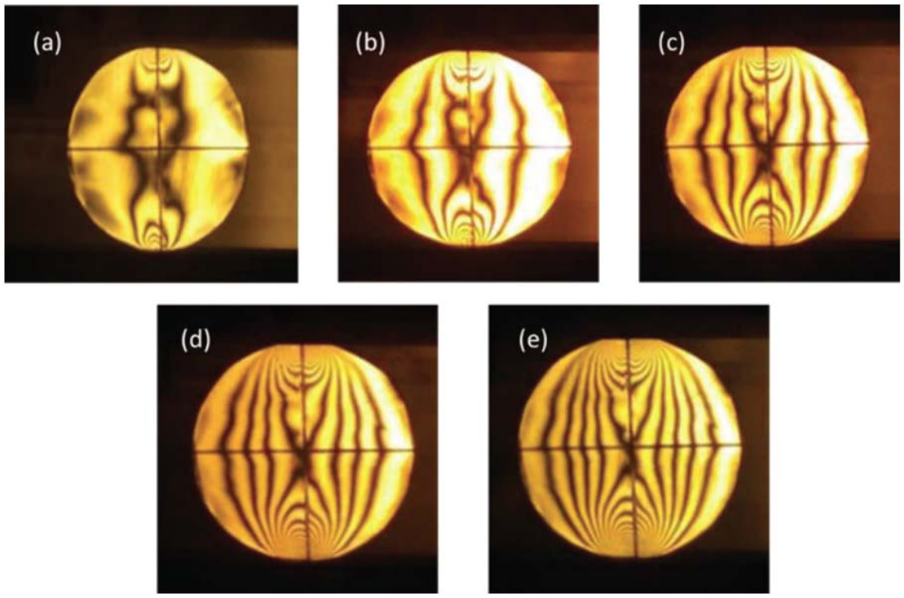

Figure 2: Isochromatic fringe pattern for F0 orientation of fibers when fringes with fringe order N= (**a**) 1, (**b**) 2, (**c**) 3, (**d**) 4 and (**e**) 5, met at the center of disc.

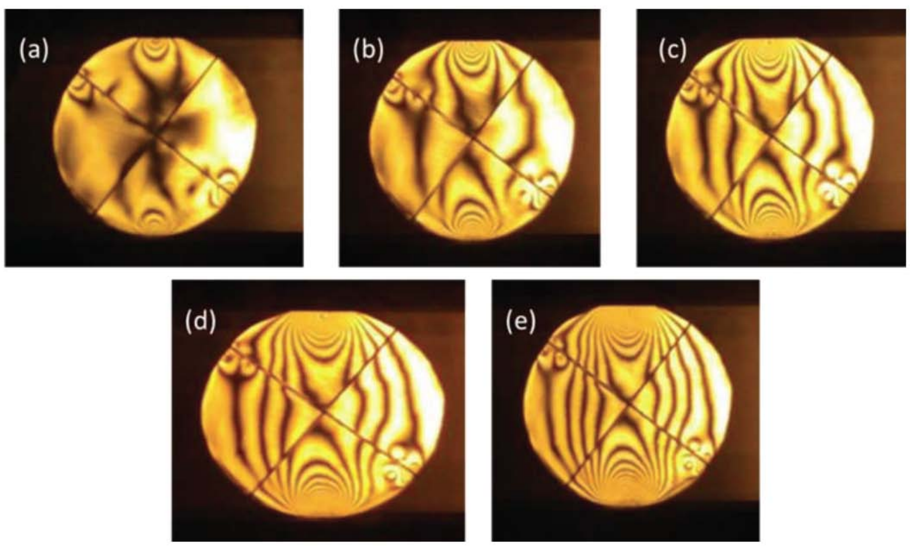

Figure 3: Isochromatic fringe pattern for F45 orientation of fibers when fringes with fringe order N= (**a**) 1, (**b**) 2, (**c**) 3, (**d**) 4 and (**e**) 5, met at the center of the disc.

with fringe order, N = 1, 2, 3, 4 and 5 met at the center of the disc. As the load was increased gradually, fringes shifted towards the circumference of the disc. The stress difference was calculated using stress optic law for respective fringe order.

3. FRINGE PATTERN AND RESULTS

Images were captured when fringes with the same fringe order met at the center of the disc. The Figures **2** and **3** shows the stress fringe pattern for F0 and F45 composite respectively, at N= 1, 2, 3, 4, and 5 (when same order fringes met at the center of the disc).

Load values were noted when fringes met the center of the disc. Material fringe values for the different orientation of fibers were calculated according to isotropic stress optic law. Let f_1 and f_2 be the material fringe values for the F0 and F45 orientation of fibers, respectively. The f_1 and f_2 were calculated to be 9.33 kN/m and 10. 88 kN/m respectively.

The load values were different for F0 and F45 when fringes of same fringe order met at the center of the disc. The load versus the fringe order is plotted in Figure **4**. It can be observed from Figure **4** that when the first order fringe met at the center of the disc, the load value was more for F45 as compared to F0. This indicated that more load was required for F45 for the onset of deformation. The variation of load with fringe order was linear for F45. Based on the average material fringe values, the stress difference was calculated at N=1, 2, 3, 4 and 5 for F0 and F45 as shown in Figure **5**.

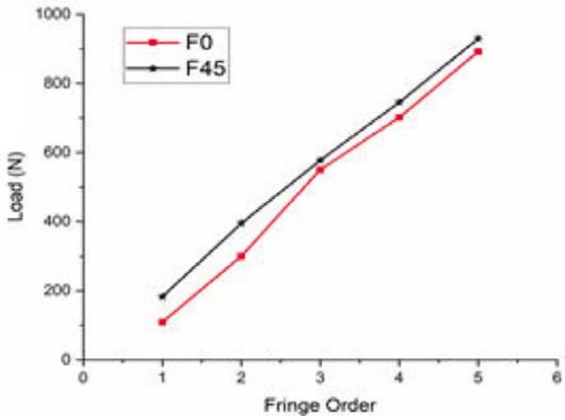

Figure 4: Load versus fringe order for F0 and F45.

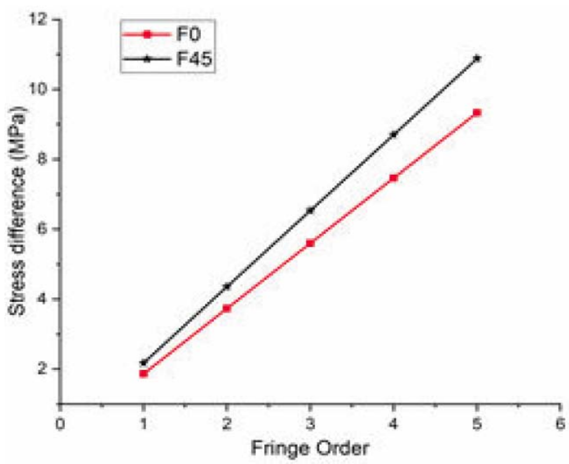

Figure 5: Load versus fringe order for F0 and F45.

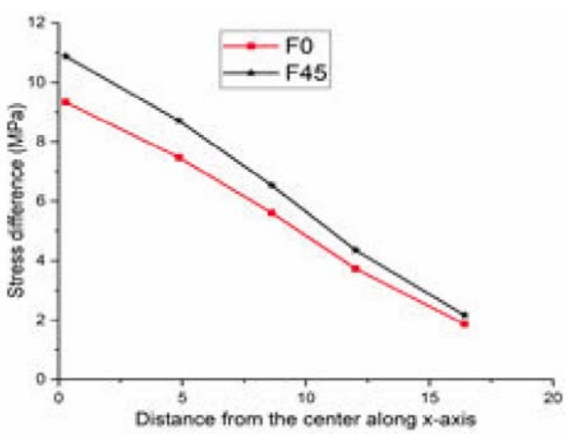

Figure 6: Comparison of stress variations for F0 and F45 along the x-axis.

To compare the effectiveness of fibers at $0^0/90^0$ and $45^0/135^0$ orientations, stresses were calculated along the x-axis at the same load level for F0 and F45, as shown in Figure **6**. It can be observed from Figure **6** that stress difference is less for F0 as compared to F45 at the same load level.

4. DISCUSSION

It can be observed from Figures **2** and **3** that fringes were distorted at the fiber/matrix interface which confirmed the strong adhesion of fiber with the matrix. As the load was increased in the case of F0, the distortion of fringes along vertical fibers reduces significantly whereas the reduction was less for horizontal fibers. This may be attributed to the load-carrying capacity of fiber in tension. Compressive load acts on the fiber in 0^0 orientation. Thus most of the load along the line of action of load is carried by the matrix in case of F0. The distortion of fringes for 90^0 orientation of fiber indicated that the indirect tensile stress was effectively resisted by fiber at 90^0.

Figure **3** shows the isochromatic fringe pattern for F45. It can be observed that isochromatic fringes were bent towards fibers which indicated that stress was effectively transferred to fibers. The distortion of fringes along both fibers indicated that both the fibers resisted shear stress induced in the material along 45^0 and 135^0.

It can be observed from Figure **4** that there was a linear relationship between load and fringe order for F45, but there was some bending for F0 at N=3. This may be attributed to the presence of fiber along the line of action of load in F0. Due to increase in load, fiber along the direction of load tries to bend in transverse direction as one or multiple half-sine waves [12]. The matrix nearby fiber resists the bending and hence increases the load due to which a curvature was observed in curve of F0 at N=3 in Figure **4**.

It can be observed from Figure **6** that along the x-axis, the stress difference corresponding to the same load level was greater when the composite was loaded in $45^0/135^0$ orientation of glass fiber with respect to loading axis as compared to $0^0/90^0$ orientation of fibers. This can be attributed to the stress sharing capacity of fibers in different orientation. In case of diametrical compression, direct compressive stress and indirect tensile stress was effectively borne by fibers in $0^0/90^0$ orientation due to their placement parallel to the stresses. However, in case of $45^0/135^0$ orientation of the fibers, there were no fibers in the direction of direct and indirect stresses. Thus, in these directions, most of the load was borne by matrix itself. Therefore, stress difference was greater in case of $45^0/135^0$ orientation of fibers.

5. CONCLUSION

In this article, photoelastic stress analysis was performed to view the stress pattern for bidirectionally glass fiber reinforced polymer composite. The isochromatic fringe pattern was observed using circular polariscope in dark-field arrangement. Two orientation of fibers (i.e. $0^0/90^0$ and $45^0/135^0$) were considered. The distortion of isochromatic fringe pattern nearby fiber/matrix interface confirmed that the inter-face was strong enough to resist the applied load. The material fringe values for $0^0/90^0$ and $45^0/135^0$ were 9.33 kN/m and 10.88 kN/m respectively. There was a little difference in the fringe values for both the orientations. This means that load carrying capacity of composite varies with the orientation of the embedded fibers.

In case of $45^0/135^0$ orientation of fibers, fringes were bent towards fibers which showed that the fibers provided a significant shear resistance. At high loads, the stress pattern for $0^0/90^0$ orientation of fibers indicated that the load share of fiber in the direction of load was very less and thus most of the load in that direction was shared by matrix only.

ACKNOWLEDGEMENT

The authors would like to acknowledge Mr. R. P. Singh, EMM laboratory, IIT (BHU) Varanasi for his help in the fabrication of specimen.

REFERENCES

[1] Ramesh M, Palanikumar K, Reddy KH. Mechanical property evaluation of sisal–jute–glass fiber reinforced polyester composites. Composites Part B: Engineering 2013; 48: 1-9. https://doi.org/10.1016/j.compositesb.2012.12.004

[2] Srivastava VK, Kumar P. Stress field around graphene nanoplates coated carbon fiber strand reinforced in polymer matrix. Materials Research Express 2019; 6: 045305. https://doi.org/10.1088/2053-1591/aafaa6

[3] Zhou X, Dai G, Guo W, Qunfang, Lin. Influence of functionalized polyolefin on interfacial adhesion of glass fiber-reinforced polypropylene. Journal of Applied Polymer Science 2000; 76(8): 1359-65. https://doi.org/10.1002/(SICI)1097-4628(20000523)76:8<1359::AID-APP17>3.0.CO;2-A

[4] Li N, Wu Z, Huo L, Zong L, Guo Y, Wang J, *et al.* One-step functionalization of carbon fiber using in situ generated aromatic diazonium salts to enhance adhesion with PPBES resins. RSC Advances 2016; 6(74): 70704-14. https://doi.org/10.1039/C6RA12717G

[5] Zhang RL, Gao B, Ma QH, Zhang J, Cui HZ, Liu L. Directly grafting graphene oxide onto carbon fiber and the effect on the mechanical properties of carbon fiber composites. Materials & Design 2016; 93: 364-9. https://doi.org/10.1016/j.matdes.2016.01.003

[6] Zhang RL, Gao B, Du WT, Zhang J, Cui HZ, Liu L, *et al.* Enhanced mechanical properties of multiscale carbon fiber/epoxy composites by fiber surface treatment with graphene oxide/polyhedral oligomeric silsesquioxane. Composites Part A: Applied Science and Manufacturing 2016; 84: 455-63. https://doi.org/10.1016/j.compositesa.2016.02.021

[7] Sakai T, Iihara Y, Yoneyama S. Photoelastic stress analysis of the fiber/matrix interface in a single-fiber composite. Journal of the Japanese Society for Experimental Mechanics 2014; 14(Special_Issue): s110-s5.

[8] Herrera-Franco PJ, Drzal LT. Comparison of methods for the measurement of fibre/matrix adhesion in composites. Composites 1992; 23(1): 2-27. https://doi.org/10.1016/0010-4361(92)90282-Y

[9] Cox H. The elasticity and strength of paper and other fibrous materials. British Journal of Applied Physics 1952; 3(3): 72. https://doi.org/10.1088/0508-3443/3/3/302

[10] Sampson RC. A stress-optic law for photoelastic analysis of orthotropic composites. Experimental Mechanics 1970; 10(5): 210-5. https://doi.org/10.1007/BF02324034

[11] Vázquez-Rodrı´guez JM, Herrera-Franco PJ, González-Chi PI. Analysis of the interface between a thermoplastic fiber and a thermosetting matrix using photoelasticity. Composites Part A: Applied Science and Manufacturing 2007; 38(3): 819-27. https://doi.org/10.1016/j.compositesa.2006.08.003

[12] Jones RM. Mechanics of composite materials: CRC press 2014.

Received on 13-09-2019 Accepted on 18-10-2019 Published on 23-10-2019

DOI: https://doi.org/10.31875/2410-4701.2019.06.5